Mathematical Statistician and Engineering Applications
ISSN:2094-0343
2326-9865

Effect of Thermal and Solutal Slip on Stagnation Point Flow of Nanofluid over a Stretching Sheet

Patil Priyanka and Jagadish V. Tawade*
Department of Mathematics, Vishwakarma University, Pune, India
***Corresponding Author:** jagadish.tawade@vupune.ac.in **(Jagadish V. Tawade)**
patilpiyu717@gmail.com (**Patil Priyanka)**

Article Info
Page Number:12698 - 12713
Publication Issue:
Vol 71 No. 4 (2022)

Article History
Article Received*: 15 September 2022*
Revised: *24 October 2022*
Accepted: *18 November 2022*
Publication: *21 December 2022*

Abstract: In this paper we analyze the effect of momentum slip, thermal slip and solutal slip on stagnation point flow of MHD nanofluid towards stretching sheet. The governing partial differential equation of flow, heat and mass transfer on considered flow are converted into the ordinary differential equations by means of similarity transformations. The resulting equations are solved by the Runge-Kutta fourth order method with efficient shooting technique. Effects of various governing parameters on flow, heat and mass transfer are studied through the plots. The various numerical tables which are calculated and tabulated. A comparison of our present results with a previous study has been done and we found that an excellent agreement is there with the earlier results and of ours.

Keywords: Nanofluid, stagnation point, Brownian motion, Thermophoresis, Heat transfer, Stretching sheet, slip parameters.

1. Introduction:

Stagnation point flow is an interesting area of research among scientists and investigators due to its importance in a wide range of applications both in industrial and scientific applications. Some of the applications are cooling of electronic devices by fans, cooling of nuclear reactors during emergency shut-down, solar central receivers exposed to wind currents, and many hydrodynamic processes in engineering applications. many investigators have extended the idea to different aspect of the stagnation point flow problems and many researchers have been working still on the stagnation point flow in various ways. Mahapatra and Gupta [1] studied two-dimensional stagnation point flow on shrinking sheet and axisymmetric stagnation point flow on an axisymmetric shrinking sheet. Lok et al. [2] numerically studied non-orthogonal stagnation point flow towards a stretching sheet using Keller-box method. It was found that the obliqueness of a free stream line causes the shifting of the stagnation point towards the incoming flow, the stagnation point flow of a micro-polar fluid towards a stretching sheet was studied by Nazar et al. [3]. Their results indicated that the solution is different from a stretching sheet, and it was found that the solutions for a shrinking sheet are not unique. Further more, Ishak et al. [4] numerically analyzed a mixed stagnation point flow of a micro-polar fluid towards a stretching sheet. They point out that micro-polar fluid showed more drag reduction characteristic when compared to classical Newtonian fluid. Similarly Hayat et al. [5] extended the problem to porous medium and investigated MHD stagnation flow of a micro-polar fluid through a porous medium. Also, Ashraf [6] incorporated the heat transfer parameter to stagnation point flow and studied MHD stagnation point flow of a micro-polar fluid towards a

heated vertical surface. Ali et al. [7] included the idea of induced magnetic field to the problem of Ashraf[6] and analyzed MHD stagnation-point flow and heat transfer towards stretching sheet with induced magnetic field. Moreover, Hayat et al.[8] They investigated the stagnation point flow towards a stretching sheet and found no boundary layer structure near the sheet . Mahapatra and Gupta [9] and reinvestigated the same stagnation point flow towards a stretching sheet and founr two kinds of boundary layer near the sheet depending on the ratio of the stretching and straining rates.

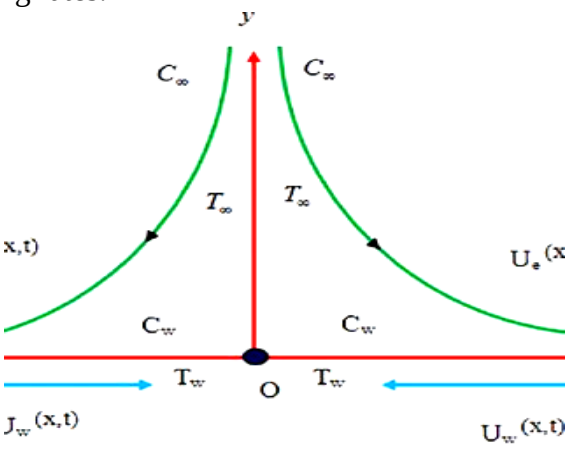

Fig. 1. Flow configuration of the problem

In this study, as shown in Fig 1, schematic diagram of two-dimensional MHD stagnation point flow over a stretching sheet.

The stagnation point flow over a stretching sheet was further investigated by Mahapatra and Gupta [10], Nazar et al [11], Layek et al. [12], Hayat et al. [13] and Zhu et al. [14,15]

On the other hand, Wang [16] first investigated the stagnation point flow towards a shrinking sheet for both two-dimensional and axisymmetric cases. Ishak et al. [17] and studied the steady boundary layer stagnation point flow of a micro-polar fluid over a shrinking sheet. Bhattacharyya and Layek [18] analyzed the effects of suction/ blowing on the boundary layer stagnation point flow and heat transfer towards a shrinking sheet in presence of thermal radiation the authors [19-25] investigated the unsteady stagnation point and heat transfer towards a shrinking sheet using HAM and Bhattacharyya [26] discussed the unsteady boundary layer stagnation point flow over a shrinking sheet using numerical method. The unsteady boundary layer flow of nanofluid over a permeable stretching /shrinking sheet is studied by Bachok et al.[27] here they studied heat transfer in the steady two dimensional stagnation point flow of a viscous fluid by taking paper by Ishak et al [28] has studied the effect of temperature dependent viscosity on mixed convection boundary layer flow and heat transfer on a continuously moving vertical surface. Local similarity solutions are obtained for the boundary layer equations subject to isothermal surface with uniform speed. By analyzing the above literature, no one studied the stagnation point flow of a nano fluid due to stretching sheet with slip effects which is very important hence this study has been carried out.

2. Mathematical Formulation:

The governing equations of flow heat and mass transfer of considered fluid are given by

$$\frac{\partial u}{\partial x}+\frac{\partial v}{\partial y}=0 \quad (1)$$

$$u\frac{\partial u}{\partial x}+v\frac{\partial u}{\partial y}=-\frac{1}{\rho f}\frac{\partial p}{\partial x}+\upsilon\left(\frac{\partial^2 u}{\partial x^2}+\frac{\partial^2 u}{\partial y^2}\right)+\frac{\sigma B_0^2}{\rho}(U_\infty-u)f \quad (2)$$

$$u\frac{\partial v}{\partial x}+v\frac{\partial v}{\partial y}=-\frac{1}{\rho f}\frac{\partial p}{\partial y}+\upsilon\left(\frac{\partial^2 v}{\partial x^2}+\frac{\partial^2 v}{\partial y^2}\right)-\frac{\sigma B_0^2}{\rho}fv \quad (3)$$

$$u\frac{\partial T}{\partial x}+v\frac{\partial T}{\partial y}=\alpha\left(\frac{\partial^2 T}{\partial x^2}+\frac{\partial^2 T}{\partial y^2}\right)+\tau D_B\left(\left(\frac{\partial \varphi}{\partial x}\frac{\partial T}{\partial x}+\frac{\partial \varphi}{\partial y}\frac{\partial T}{\partial y}\right)\frac{D_T}{T_\infty}\left[\left(\frac{\partial T}{\partial x}\right)^2+\left(\frac{\partial T}{\partial y}\right)^2\right]\right) \quad (4)$$

$$u\frac{\partial \varphi}{\partial x}+v\frac{\partial \varphi}{\partial y}=D_B\left(\frac{\partial^2 \varphi}{\partial x^2}+\frac{\partial^2 \varphi}{\partial y^2}\right)+\frac{D_T}{T_\infty}\left(\frac{\partial^2 T}{\partial x^2}+\frac{\partial^2 T}{\partial y^2}\right) \quad (5)$$

Where u and v are velocity components along x and y- axis υ is the kinematics viscosity ρ_f is the density of the base fluid, σ electrical conductivity U_∞, B_0, ρp, $(\rho c)_f$, D_B and D_T are the free stream velocity, , magnetic field, the density of the nanoparticle, heat capacity of a base fluid, the Brownian diffusion and thermophoretic diffusion coefficient respectively, and $\alpha=\frac{k}{(\rho c)_f}, \tau=\frac{(\rho c)_p}{(\rho c)_f}, \upsilon=\frac{\mu}{\rho f}$. . Where V= (u, v),$\rho_{nf}$,$\mu_{nf}$, $k_{nf,}$, and β_{nf} are the density, the thermal conductivity, and the volumetric volume expansion coefficient of the nanofluid, respectively, which are defined as:

Thermophysical Properties of nanofluids are given by

$$\left.\begin{aligned}\rho_{nf}&=(1-\varphi)\rho_f+\varphi\rho_p\\ \mu_{nf}&=\frac{\mu_f}{(1-\varphi)^{2.5}}\\ (\rho\beta)_{nf}&=(1-\varphi)_f+\varphi(\rho\beta)_p\\ \alpha_{nf}&=\frac{k_{nf}}{(\rho c_p)_{nf}}\end{aligned}\right\} \quad (6)$$

$$(\rho c_p)_{nf}=(1-\phi)(\rho c_p)_f+\phi(\rho c_p)_p \quad (7)$$

$$\frac{k_{nf}}{k_f}=\frac{k_p+2k_f-2\phi(k_f-k_p)}{k_p+2k_f+2\phi(k_f-k_p)} \quad (8)$$

ϕ is the Solid volume fraction, T is the temperature inside the boundary layer, $(\rho c)_p$effective heat capacity of a nanofluid, and μ.g is the acceleration due to gravity. μ_f is the dynamic viscosity of the base fluid, β_f and β_p are the thermal expansion coefficients of the base fluid and the nanoparticle, respectively, and $\beta_p$are the densities of the nanoparticle, the suffixes f, p, and nf denote base fluid, nanoparticle, and nanofluid conditions, respectively, and $(\rho c_p)_{nf}$ is the heat capacitance of the nanofluid,

Where k_f and $kp$are the thermal conductivities of the base fluid and nanoparticle, respectively.

The boundary conditions are:

$$\left.\begin{array}{l} u - u_w(x) = L\frac{\partial u}{\partial y}, \quad v = 0, \quad T - T_w(x) = k_1\frac{\partial T}{\partial y}, \; C - C_w(x) = k_2\frac{\partial C}{\partial y} \quad \text{at } y = 0, \\ u \to 0, \qquad T \to T_\infty, \quad C \to C_\infty \quad as \qquad y \to \infty, \\ \text{Where} \quad u_w(x) = \alpha x, \qquad T_w(x) = T_\infty + b(\frac{x}{l}) \text{ and } \qquad C_w(x) = C_\infty + c(\frac{x}{l}). \\ \text{Using the transformation} \\ u = \alpha x f'(\eta), v = -\sqrt{\alpha \upsilon} f(\eta), \quad \frac{T - T_\infty}{T_W - T_\infty} = \theta(\eta), \quad h(\eta) = \frac{\varphi - \varphi_\infty}{\varphi_W - \varphi_\infty} \\ \text{Where } \eta = \sqrt{\frac{\alpha}{\upsilon}}\, y, \end{array}\right\} \quad (9)$$

Using an order magnitude analysis of the y-direction momentum equation (normal to the sheet) using the usual boundary layer approximation:

$$\left.\begin{array}{c} u >> v \\ \frac{\partial u}{\partial y} >> \frac{\partial v}{\partial x}, \frac{\partial v}{\partial x}, \frac{\partial v}{\partial y} \\ \frac{\partial p}{\partial y} = 0 \end{array}\right\} \quad (10)$$

After boundary layer approximation, the governing equations are reduced to

$$\frac{\partial u}{\partial x} + \frac{\partial v}{\partial y} = 0 \quad (11)$$

$$u\frac{\partial u}{\partial x} + v\frac{\partial u}{\partial y} = U_\infty \frac{\partial U_\infty}{\partial x} + \upsilon(\frac{\partial^2 u}{\partial y^2}) + \frac{\sigma B_0^2}{\rho}(U_\infty - u)f \quad (12)$$

$$u\frac{\partial T}{\partial x} + v\frac{\partial T}{\partial y} = \alpha(\frac{\partial^2 T}{\partial y^2}) + \tau\{D_B(\frac{\partial h}{\partial y}\frac{\partial T}{\partial y})\frac{D_T}{T_\infty}[(\frac{\partial T}{\partial y})^2]\} \quad (13)$$

$$u\frac{\partial \varphi}{\partial x} + v\frac{\partial \varphi}{\partial y} = D_B(\frac{\partial^2 h}{\partial y^2}) + \frac{D_T}{T_\infty}(\frac{\partial^2 T}{\partial y^2}) \quad (14)$$

The boundary conditions are also reduced

$$u - u_w(x) = L\frac{\partial u}{\partial y}, \quad v = 0, \quad T - T_w(x) = k_1\frac{\partial T}{\partial y}, \; C - C_w(x) = k_2\frac{\partial C}{\partial y} \quad \text{at } y = 0,$$

$$u \to 0, \qquad T \to T_\infty, \quad C \to C_\infty \quad as \qquad y \to \infty,$$

Where $u_w(x) = \alpha x, \qquad T_w(x) = T_\infty + b(\frac{x}{l})$ and $\qquad C_w(x) = C_\infty + c(\frac{x}{l}).$ (15)

We now introduce the following dimensionless quantities; ie similarity transformations used to reduce given partial differential equations to ordinary differential equations.

$$\eta = \sqrt{\frac{\alpha}{\upsilon}}\, y, \quad \psi = -\sqrt{\alpha \upsilon x} f(\eta), \theta(\eta) = \frac{T - T_\infty}{T_W - T_\infty}, \; h(\eta) = \frac{\varphi - \varphi_\infty}{\varphi_W - \varphi_\infty} \quad (16)$$

The equations of continuity is satisfied if we choose a stream function ψ (xy) such that

$$u = \frac{\partial \psi}{\partial y}, \qquad v = -\frac{\partial \psi}{\partial x} \quad (17)$$

Using the similarity transformation quantities, the governing equations (11). (12), (13) and (14) are transformed to the ordinary differential equation as follows:

$$f''' + ff'' - f'^2 + M(A - f') + A^2 = 0 \quad (18)$$

$$\theta'' + Pr\, f\, \theta' + Pr\, N\, b h' \theta' + Pr\, N\, t\theta'^2 = 0 \quad (19)$$

$$h'' + Lefh' + \frac{Nt}{Nb}\theta'' = 0 \quad (20)$$

With the boundary conditions

$$f(0) = 0,\ f'(0) = 1 + \beta f''(0), \theta(0) = 1 + \gamma\theta'(0), h(0) = 1 + \delta\varphi'(0),\ \text{at}\ \eta \to 0$$
$$f'(\infty) = A, \qquad \theta(\infty) = 0, \qquad h(\infty) = 0, \quad \text{as} \quad \eta \to \infty \quad (21)$$

Where the six governing parameters are defined as:

$$\Pr = \frac{\nu}{b}, A = \frac{b}{a}, M = \frac{\sigma B_0^{\,2}}{\rho_f a},\ Le = \frac{\nu}{D_B}$$
$$Nt = \frac{(\rho C)_p D_T (T_w - T_\infty)}{(\rho C)_f \nu T_\infty}, Nb = \frac{(\rho C)_p D_B (\phi_w - \phi_\infty)}{(\rho C)_f \nu} \quad (22)$$

Where f', θ and h are the dimensionless velocity, temperature and particle concentration with respect to η is the similarity variables, the prime denotes differentiation with respect to η. ***Pr, A, M, Nb, Nt, Le*** denotes a Prandtl number, and a velocity ratio, a magnetic parameter, a Brownian motion parameters, a thermophoresis parameter, and a Lewis number, respectively. The important physical quantities of interest in this problem are the skin friction coefficient cf , local Nusselt number Nu_x and the local Sherwood number Sh_x are defined as:

$$c_f = \frac{\tau_w}{\rho(u_w)^2}, \quad Nu_x = \frac{x q_w}{k(T_w - T_\infty)}, \ Sh_x = \frac{x h_m}{D_B(\varphi_w - \varphi_\infty)} \quad (23)$$

Where the skin friction τ_w, wall heat flux qw and wall mass flux q_w are given by

$$\tau_w = \mu\left(\frac{\partial u}{\partial y}\right)_{y=0}, \qquad q_w = -k\left(\frac{\partial T}{\partial y}\right)_{y=0}, \qquad h_m = -D_B\left(\frac{\partial \varphi}{\partial y}\right)_{y=0} \quad (24)$$

By using the above equations, we get

$$c_f\sqrt{Re_x} = f''(0\ \ \frac{Nu_x}{\sqrt{Re_x}} = -\theta'(0), \frac{Sh_x}{\sqrt{Re_x}} = -h'(0) \quad (25)$$

where Re_x Nu_x , Sh_x are local Reynolds number, local Nusselt number and local Sherwood number, respectively.

3. Numerical Solution:

In this study, an efficient Runge-kutta fourth order method along with shooting technique has been used to analyze the flow model of coupled ordinary differential equations Eq.(18)-(20) for different values of governing parameters viz. prandtl number Pr, velocity ratio parameter A, a Brownian motion parameter Nt and a Lewis number Le. The coupled ordinary differential equations (18)-(20) are third order in f and second order in both θ and h respectively which have been reduced to a system of seven simultaneous equations for seven unknown. In order to solve numerically this system of equations using Range-kutta method, we require seven initial conditions but two initial conditions in f one initial condition in each of θ and h are known. However, the values of f', θ and h are known at η→∞. Thus,

these three end conditions are utilized to produce two unknown initial conditions at η= 0 by using shooting technique.

The Eqs. (18)-(20) can be expressed as

$$f''' = -ff'' + f'^2 - M(A - f') - A^2 \quad (26)$$

$$\theta'' - Pr\, f\, \theta' - Pr\, N\, b h' \theta' - Pr\, N\, t \theta'^2 \quad (27)$$

$$h'' = -Lef h' - \frac{Nt}{Nb}\theta'' \quad (28)$$

Now defining new variables by the equation

$$f_1 = f, f_2 = f', \; f_3 = f'', \; f_4 = \theta, \; f_5 = \theta', \; f_6 = h, \; f_7 = h', \quad (29)$$

The three coupled higher order differential equations and the boundary conditions may be transformed to seven equivalent first order differential equations and boundary conditions respectively as given below: Using Eq.(29) we can write the initial value problem as follows:

$$f_1' = f_2, \; f_2' = f_3, \; f_3' = -f_1 f_3 + f_2^2 - M(A - f_2) - A^2, \; f_4' = f_5,$$
$$f_5' = -Pr\, f_1 f_5 - Pr\, N\, b f_5 f_7 - Pr\, N\, t f_5^2, \; f_6' = f_7, \quad (30)$$
$$f_7' = -Le + \frac{Nt}{Nb}(Pr\, f_1 f_5 + Pr\, N\, b f_5 f_7 + Pr\, N\, t f_5^2)$$

A prime denote the differentiation with respect to η and the boundary conditions are Here prime denotes the differentiation with respect to and the initial conditions in Eq.(21) become as follows:

$$f_1' = 0, f_2' = 0, \; f_3' = p, f_4' = 1, f_5' = q, f_6' = 1, \; f_7' = r \quad (31)$$

Here we need to solve a sequence of initial value problems as above, by taking α=α_n, β=β_n and $\gamma = \gamma_n$, so that the end boundary values thus obtained numerically match up to desired degree of accuracy with the boundary values at ∞ given in the problem. In what follows, $f_i(\infty, \alpha, \beta, \gamma)$ is the solution at infinity to be obtained by the classical Runge-kutta method for unknown slopes. Let us assume the initial value problem satisfies necessary conditions for existence and uniqueness of solutions, the problem now reduces to that of finding α, β and γ such that:

$$F(p,q,r) = f'(\infty, p, q, r) - f'(\infty) = f_2(\infty, p, q, r) - f_2(\infty) = 0$$
$$\Theta(p,q,r) = \theta(\infty, p, q, r) - \theta(\infty) = f_4(\infty, p, q, r) - f_4(\infty) = 0$$
$$H(p,q,r) = h(\infty, p, p, r) - h(\infty) = f_6(\infty, p, q, r) - f_6(\infty) = 0 \quad (32)$$

These are three non-linear equations in p, q and r which are to be solved by Newton-Rephson method. This method for finding roots of non-linear equations, with p_0, q_0 and r_0 as initial values, which yields the following iterative scheme:

$$\begin{bmatrix} p_{n+1} \\ q_{n+1} \\ r_{n+1} \end{bmatrix} = \begin{bmatrix} p_n \\ q_n \\ r_n \end{bmatrix} - \begin{bmatrix} \frac{\partial F}{\partial p} & \frac{\partial F}{\partial q} & \frac{\partial F}{\partial r} \\ \frac{\partial \theta}{\partial p} & \frac{\partial \theta}{\partial q} & \frac{\partial \theta}{\partial r} \\ \frac{\partial H}{\partial p} & \frac{\partial H}{\partial q} & \frac{\partial H}{\partial r} \end{bmatrix}^{-1}_{p_n, q_n, r_n} \begin{bmatrix} F \\ \Theta \\ H \end{bmatrix}_{p_n, q_n, r_n} \quad (33)$$

Where n=0,1,2,3……

To implement the scheme (33) we require finding the nine partial derivatives in the to be inverted matrix. These can be obtained by differentiating the initial value problem, given in Eq.(30)-(31) with

respect to p, q and r. By differentiating Eq.(30)-(31) with respect to p, q and r we get three more initial value problem known as variational equations. On solving some initial value problems, it is possible to go ahead with iterative scheme (33).

The accuracy chosen for obtaining p, q and r Newton-Raphson method was 10^{-7} . convergence of Newton-Raphson iterative scheme was ensured due to the scientific choice of missing initial values there by circumventing the usual problem of slow convergence or divergence or overflow encountered in shooting method procedures. Here we also note that, the governing ODEs of stretching sheet problems are not stiff and hence we do not need procedures

4. Results and Discussion:

After solving the final ordinary differential equations we obtain the results which are explained below through the plots.

Fig.2 illustrates the influence of velocity ratio parameter A on velocity graph. When the free stream velocity exceeds the velocity of the stretching sheet, the flow velocity increases the boundary layer thickness decrease with increase in A. Moreover, when the free stream velocity less than stretching velocity, the flow flied velocity decreases and boundary layer thickness also decreases. When A>1, the flow has a boundary layer structure and boundary thickness decreases as a values of A increases. On the other hand, when A<1, the flow has an inverted boundary layer structure, for this case also, as the values A decrease the boundary layer thickness decreases.

Fig.3 shows that the presence of transverse magnetic field sets in Lorentz force, which results in retarding force on the velocity field. Therefore, as the values of M increases does the retarding force and hence the velocity decreases. When A=3.3 i.e b/a>1, the flow has boundary layer structure and the boundary layer thickness decreases as the value of M increases.

Figure 4 shows the influence of the change of Brownian motion parameter Nb and thermophoresis parameter Nt on temperature profile It is noticed that as thermophoresis parameter increases the thermal boundary layer thickness increases and the temperature gradient at the surface decrease (in absolute value) as both Nb and Nt increase.

Figure 5 shows that the variation of temperature profile in response to a change in the values of velocity ratio parameter A. It is seen that as velocity ratio parameter increases the thermal boundary layer thickness decreases.

Figure 6 represents the variation of temperature graph with respect to Prandtl number Pr. The graph depicts that the temperature decreases when the value of Prandtl number Pr increase at a fixed value η. This is due to the fact that a higher Prandtl number fluid has relatively low thermal conductivity, which reduces conduction and thereby the thermal; boundary layer thickness; and as a result, temperature decreases. Increasing pr is to increase the heat transfer rate at surface because the temperature gradient at the surface increases. The influence of Prandtl on Newtonian fluids is similar to what we observed in nanofluid. Therefore, these properties are also inherited by nanofluids.

Figure 7 depicts the influence of velocity ratio parameter A on concentration graph. As the value of A increase, the concentration boundary layer thickness decreases. Moreover, it is possible to recognize from the graph that the magnitude of temperature gradient on the surface of a plate increase as A increases. As it is noticed from fig- 8, as Lewis number increases the concentration graph decreases. Moreover, the concentration boundary layer thickness decreases as

Lewis number increase. This is probably due to the fact mass transfer rate increases as Lewis number increases. It also reveals that the concentration gradient at surface of the plate increases.

The plot 9 reveals variation of concentration graph in response to a change in Brownian motion parameter Nb. The influence of Brownian motion on concentration profile graph is as the value of Brownian motion parameter increase, the concentration boundary layer thickness is decreasing. The graph also reveals that the thermal boundary layer thickness doesn't change much when the values of Nb increases.

Figure 10 represents a variation of skin friction coefficient f'' (0) with respect to magnetic field parameter M and velocity ratio parameter A. the magnitude of skin friction coefficient f'' (0) increases with increasing M for both cases A>1 and A<1. when A=1 the graph has is a constant value to zero. The zero friction for the case A=1 indicate that the sheet and the fluid moves with the same velocity.

Figure 11 demonstrate the variation of local Nusselt number - θ(0) with respect to M for different values velocity ratio parameter A. from the graph we notice that - θ'(0) increases as M increases for A>1, but it decreases with M for A<1. when A=1 the values of - θ'(0) remains constant i.e - θ'(0)= 0.4767≠0 which means there is a heat transfer between the sheet and fluid even though the skin friction coefficient for this case is zero (see.fig12) since the sheet and fluid are at different temperature.

Figures 12 and 13 depicts the variation of local Sherwood number - h'(0) in response to a change in both Lewis number Le and velocity ratio parameter A. It is notice from fig 15 that the local Sherwood number graph increases as both parameters increase.

Figs 14, 15 and 16 show the effect of momentum slip on velocity profile, thermal slip on temperature profile and solutal slip on mass transfer profile respectively, temperature profile and concentration profile decreases with increase in parametric values. But opposite result observed in velocity profile.

Table 1: comparison of values of *f*'' (0) with previous result when M=0

A	Present Result	Ibrahim et al	Mahapatra[1]	Hayat[7]
0. 01	-0.9980	-0.9980	-	-0.99823
0.1	-0.9693	-0.9694	-0.9694	-0.96954
0.2	-0.9181	-0.9181	-0.9181	-0.91813
0.5	-0.6672	-0.6673	-0. 6673	-0.66735
2.0	2.0174	2.0175	2.0175	2.01767
3.0	4.7293	4.7292	4.7293	4.72964

Pr	A	Present Result	Ibrahim et al	Mahapatra[1]	Hayat[7]
1	0.1	0.6021	0.6022	0.603	0.602156
	0.2	0.6244	0.6245	0.625	0.624467
	0.5	0.6924	0.6924	0.692	0.692460
1.5	0.1	0.7768	0.7768	0.777	0.776802
	0.2	0.7971	0.7971	0.797	0.797122
	0.5	0.8647	0.8648	0.863	0.864771

Table 2: Comparison of local Nusselt number - θ'(0) at Nt=0, Nb→0, for different values of with previously published data

The table 1 and 2 show the comparison study of our results with earlier work there is a good agreement between our and pervious results With table 1 earlier work.

5. Conclusion

On investigation of nano fluid flow due to stagnation point flow, we came to the following conclusions, which are

1. Velocity profiles graph increase with an increases in A when A>1.
2. The thickness of velocity boundary layer decreases with an increase in magnetic field parameter M.
3. Thermal boundary layer thickness decreases with an increase in both velocity ratio parameter A and Prandtl number Pr.
4. The thickness of thermal boundary layer increases with an increase in both Nt= Nb parameter.
5. The magnitude of the skin friction coefficient f''(0) increases with M when A≠1and it is zero when A=1
6. An increase in velocity ratio parameter A increases both the local Nusselt number and Local Sherwood number.
7. An increase in magnetic parameter M increases both the local Nusselt number - θ'(0) and local Sherwood number - h'(0).
8. When the value of velocity ratio parameter A=1, the skin friction coefficient, local Nusselt number and local Sherwood number all are constant.
9. The wall temperature gradient increases with an increase in Lewis number Le and Prandtl number Pr.

Nomenclature:

A	velocity ratio parameter
B_0	magnetic field strength
c_f	skin friction coefficient
c_w	concentration at the surface of the sheet
c_∞	ambient concentration
D_B	Brownian diffusion coefficient
D_T	thermophoresis diffusion coefficient
f	dimensionless stream function
h	dimensionless concentration function
k	thermal conductivity
Le	Lewis number
M	magnetic parameter
Nb	Brownian motion parameter
Nt:	thermophoresis parameter
Nu_x	local Nusselt number
Pr	Prandtl number
Re_x	local Reynolds number
T:	temperature of the fluid inside the boundary layer
Sh_x	local Sherwood number
T_w	temperature at the surface of the sheet
T_∞	ambient temperature
U_∞	free stream velocity
u,v	velocity component along x- and y-direction

Greek symbols

η	dimensionless similarity variable
μ	dynamic viscosity of the fluid
υ	kinematic viscosity of the fluid
$(\rho)_f$	density of the basefluid
$(\rho c)_f$	heat capacity of the base fluid
$(\rho c)_p$	effective heat capacity of a nanoparticle(qc)
ψ	stream function
α	thermal diffusivity
σ	electrical conductivity
Θ	dimensionless temperature
τ	parameter defined by $\frac{(\rho c)_p}{(\rho c)_f}$

Subscripts

∞	condition at the free stream
W	condition at the surface

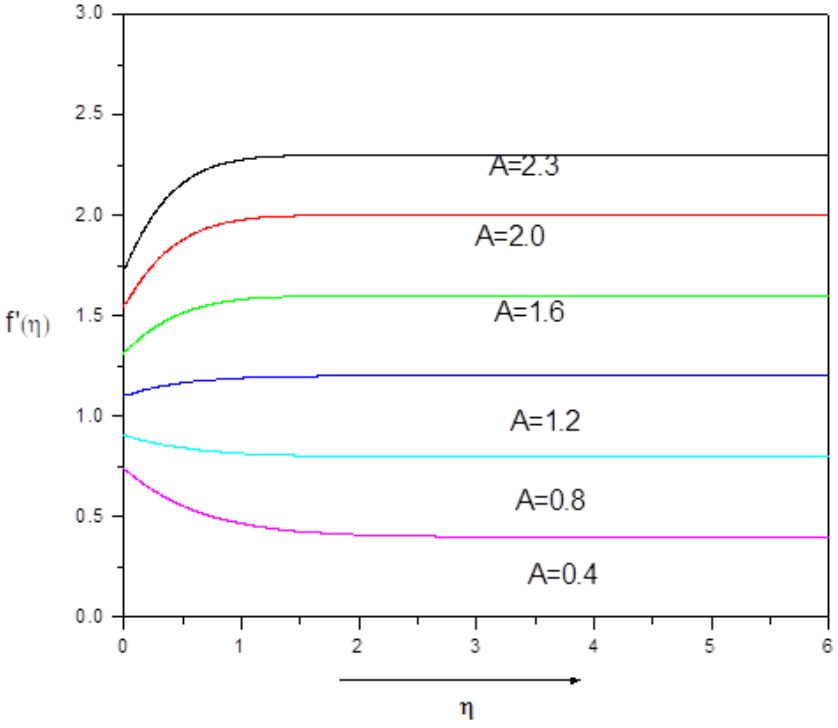

Fig.2 Influence of velocity ratio parameter A on the velocity profile

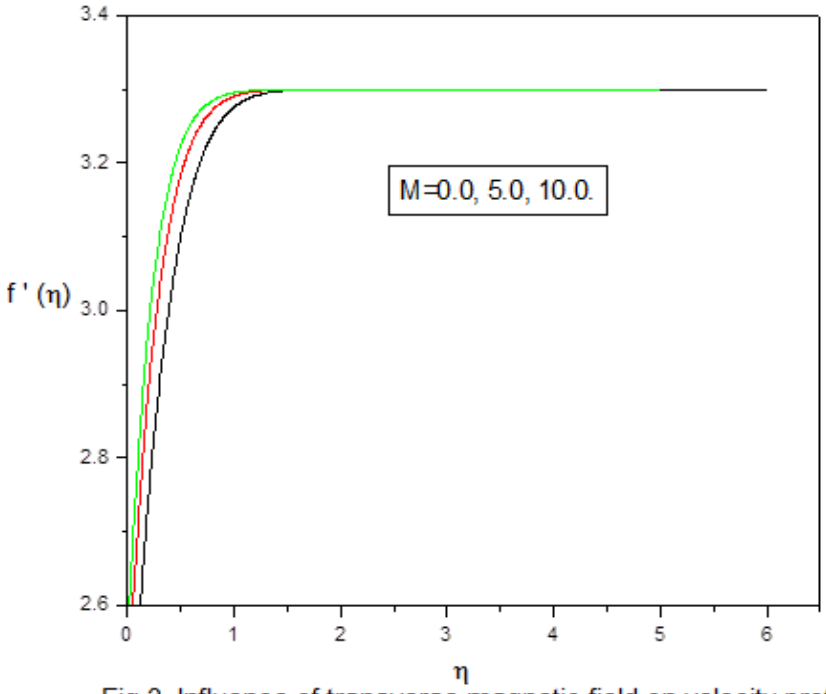

Fig.3. Influence of transverse magnetic field on velocity profile

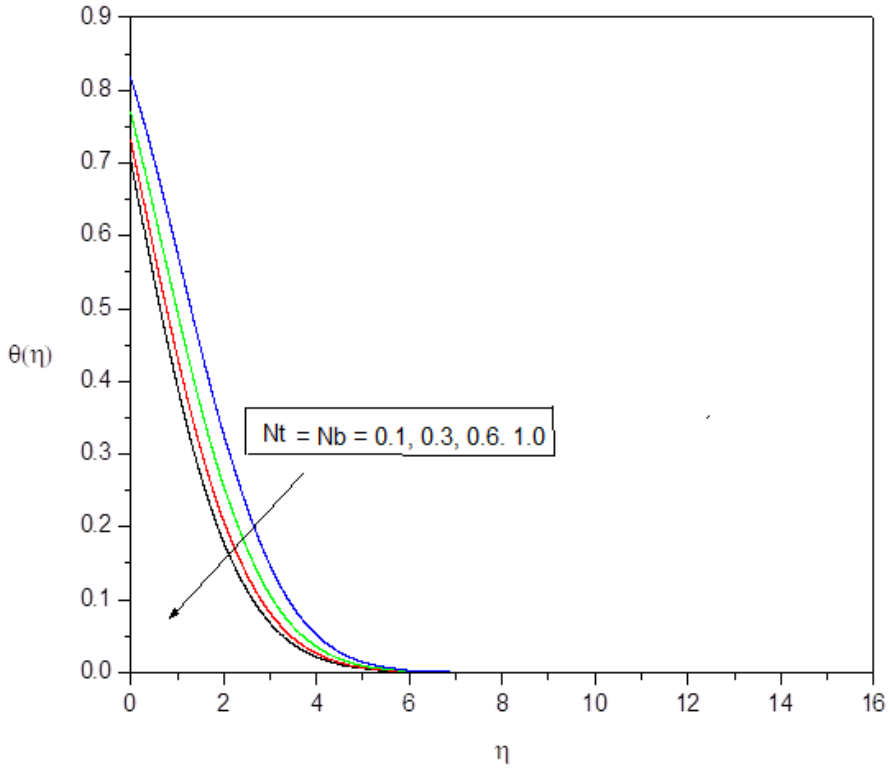

Fig.4. Influence of Brownian motion parameter Nb and thermophoresis parameter Nt on the temperature profile

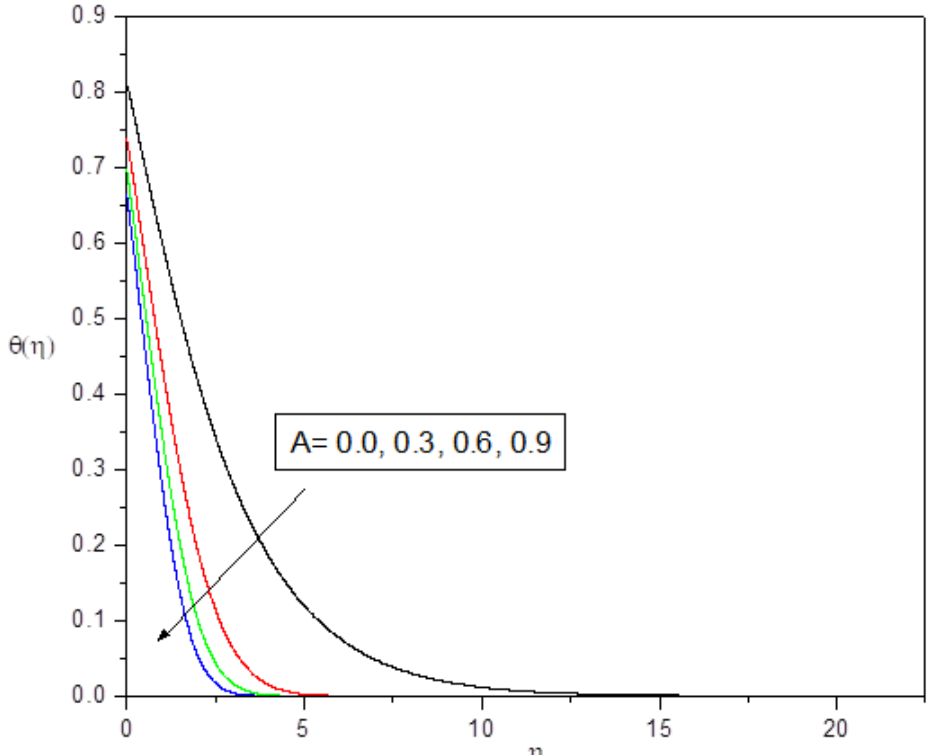

Fig. 5: Influence of temperature profile Vs velocity ratio parameter A.

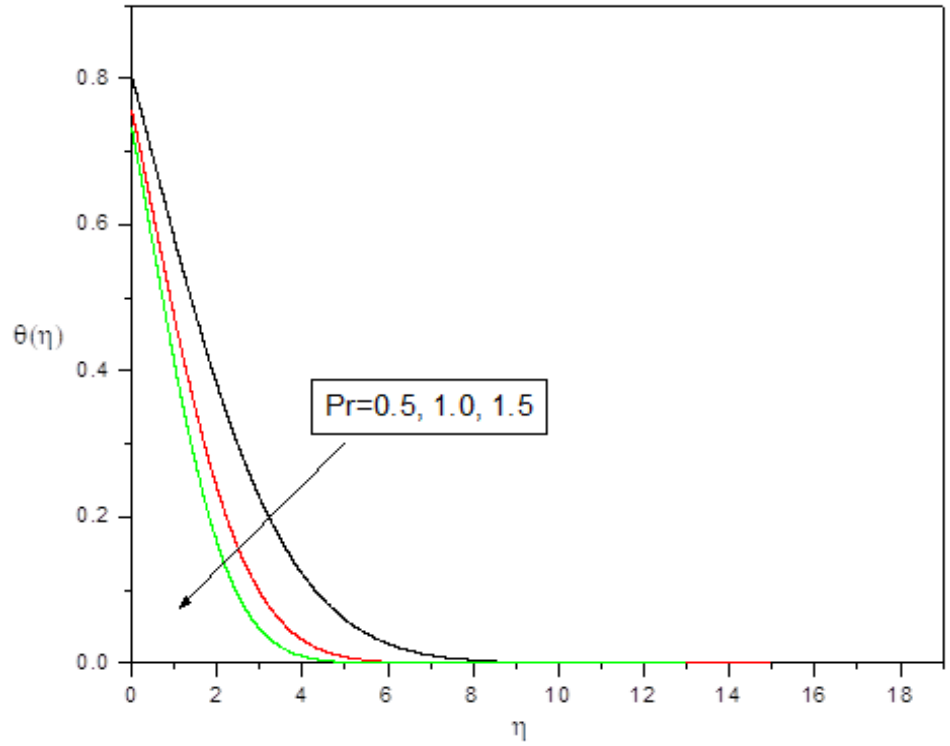

Fig.6. Influence of temperature profile Vs Prandtl number Pr.

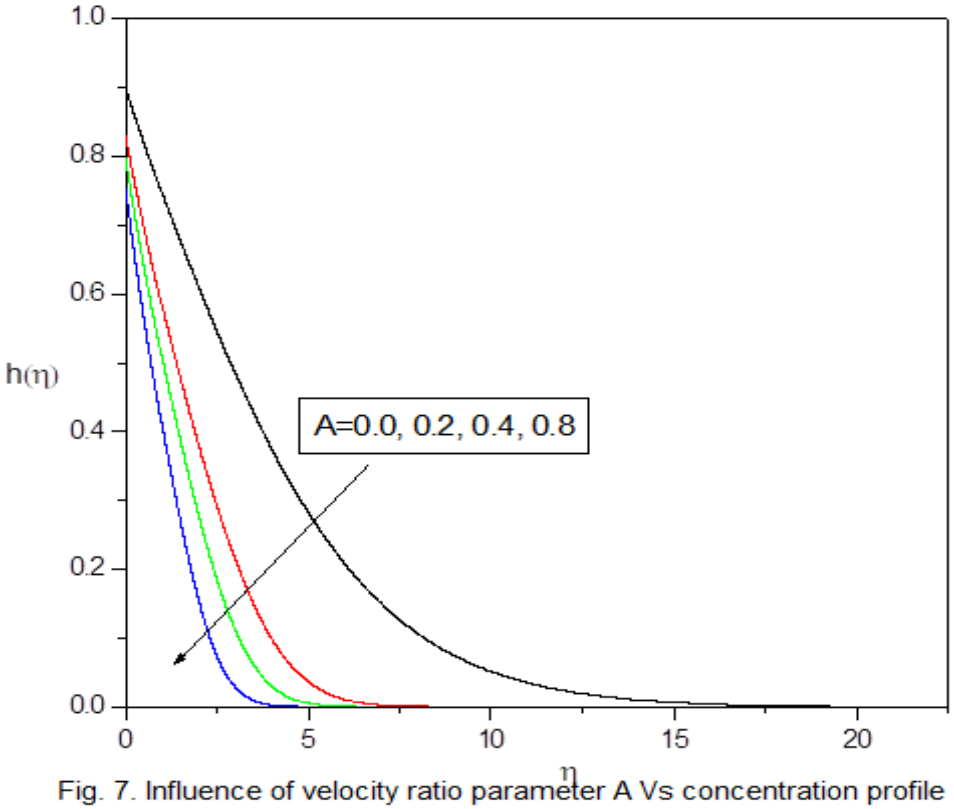

Fig. 7. Influence of velocity ratio parameter A Vs concentration profile

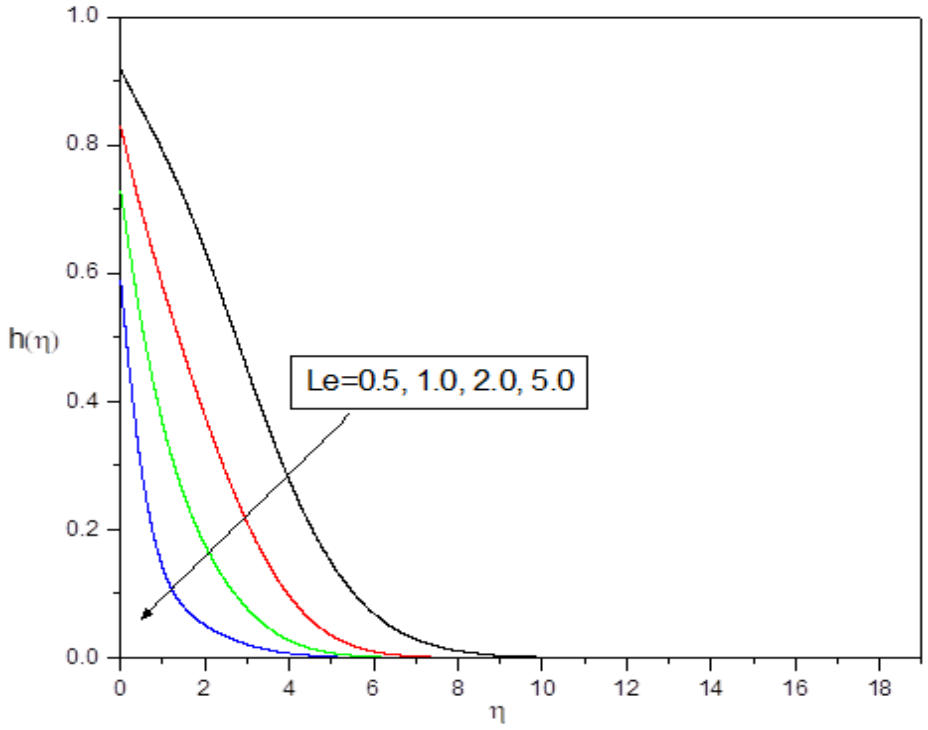

Fig. 8. Influence of Lwin number Vs concentration profile

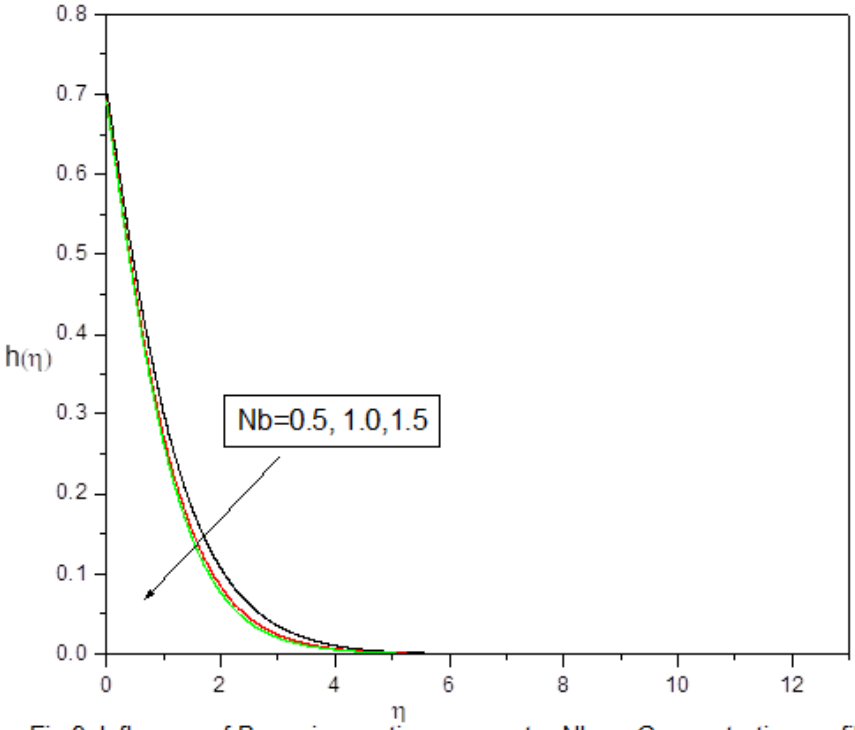

Fig.9. Influence of Brownian motion parameter Nb on Concentration profile

References:

[1] T.R. Mahapatra, A.G. Gupta, Heat transfer in stagnation point flow towards a stretching sheet, Heat Mass Transfer 38 (2002) 517–521.

[2] Y.Y. Lok, N. Amin, I. Pop, Non-Orthogonal stagnation point flow towards a stretching sheet, Int. J. Non-Linear Mech. 41 (2006) 622–627.

[3] R. Nazar, N. Amine, D. Filip, I. Pop, Stagnation point flow of a microploar fluid towards a stretching sheet, Int. J. Non-Linear Mech. 39 (2004) 1227–1235.

[4] A. Ishak, R. Nazar, I. Pop, Mixed convection stagnation point flow of a micropolar fluid towards a stretching sheet, Mechanica 43 (2008) 411–418.

[5] T. Hayat, T. Javed, Z. Abbas, MHD flow of a micropolar fluid near a stagnation-point towards a non-linear stretching surface, Non-Linear Analysis: Real World Applications 10 (2009) 1514–1526.

[6] M. Ashraf, M.M. Ashraf, MHD stagnation point flow of a micropolar fluid towards a heated surface, Appl. Math. Mech. -Engl. Ed. 32 (1) (2011) 45–54.

[7] F.M. Ali, R. Nazar, N.M. Arifin, I. Pop, MHD stagnation-point flow and heat transfertowards stretching sheet with induced magnetic field, Appl. Math Mech. -Engl. Ed. 32 (4) (2011) 409–418.

[8] T. Hayat, A. Rafique, M.Y. Malik, S. Obaidat, Stagnation-point flow of maxwell fluid with magnetic field and radiation effects, Heat Transfer – Asian Research 41 (1) (2012) 23–32.

[9] Mahapatra TR, Gupta AS. Magnetohydrodynamic stagnation point flow towards a stretching sheet. Acta Mech 2001;152:191–6.

[10] Mahapatra TR, Gupta AS. Heat transfer in stagnation-point flow towards a stretching sheet. Heat Mass Transfer 2002;38:517–21.

[11] Nazar R, Amin N, Filip D, Pop I. Stagnation point flow of a micropolar fluid towards a stretching sheet. Int J Non-Linear Mech 2004;39:1227–35.
[12] Layek GC, Mukhopadhyay S, Samad SKA. Heat and mass transfer analysis for boundary layer stagnation-point flow towards a heated porous stretching sheet with heat absorption/generation and suction/blowing. Int Commun Heat Mass Transfer 2007;34:347–56.
[13] Hayat T, Javed T, Abbas Z. MHD flow of a micropolar fluid near a stagnation-point towards a non-linear stretching surface. Nonlinear Anal Real World Appl 2009;10:1514–26.
[14] Zhu J, Zheng L, Zhang X. Homotopy analysis method for hydromagnetic plane and axisymmetric stagnation-point flow with velocity slip. WASET 2010;63:151–4.
[15] Zhu J, Zheng L, Zhang ZG. Effects of slip condition on MHD stagnation-point flow over a power-law stretching sheet. Appl Math Mech 2010;31:439–48.
[16] Wang CY. Stagnation flow towards a shrinking sheet. Int J Nonlinear Mech 2008;43:377–82.
[17] Ishak A, Lok YY, Pop I. Stagnation-point flow over a shrinking in a micropolar fluid. Chem Eng Commun 2010;197:1417–27.
[18] Bhattacharyya K, Layek GC. Effects of suction/blowing on steady boundary layer stagnation-point flow and heat transfer towards a shrinking sheet with thermal radiation. Int J Heat Mass Transfer 2011;54:302–7.
[19] Bhattacharyya K, Mukhopadhyay S, Layek GC. Slip effects on boundary layer stagnation-point flow and heat transfer towards a shrinking sheet. Int J Heat Mass Transfer 2011;54:308–13.
[20] Lok YY, Ishak A, Pop I. MHD stagnation-point flow towards a shrinking sheet.
[21] Int J Numer Meth Heat Fluid Flow2011;21:61–72.
[22] Mahapatra TR, Nandy SK, Gupta AS. Momentum and heat transfer in MHD stagnation-point flow over a shrinking sheet. ASME J Appl Mech 2011;78:021015.
[23] Yacob NA, Ishak A, Pop I. Melting heat transfer in boundary layer stagnation-point flow towards a stretching/shrinking sheet in a micropolar fluid. Comput Fluids 2011;47:16–21.
[24] Bhattacharyya K. Dual solutions in boundary layer stagnation-point flow and mass transfer with chemical reaction past a stretching/shrinking sheet. Int Commun Heat Mass Transfer2011;38:917–22.
[25] Rosali H, Ishak A, Pop I. Stagnation point flow and heat transfer over a stretching/
A. shrinking sheet in a porous medium. Int Commun Heat Mass Transfer 2011;38:1029–32.
B. Bhattacharyya K, Vajravelu K. Stagnation-point flow and heat transfer over an exponentially shrinking sheet. Commun NonlinearSci Numer Simul 2012; 17:2728–34.
[26] Bhattacharyya K. Dual solutions in unsteady stagnation-point flow over a shrinking
A. sheet. Chin Phys Lett 2011;28:084702.
[27] Bachok N, Ishak A, Pop I. Unsteady boundary-layer flow and heat transfer of a
A. nanofluid over a permeable stretching/shrinking sheet. Int J Heat Mass Transfer 2012;55:2102–9.
[28] Ishak, R. Nazar, I. Pop, Mixed convection boundary layers in the stagnation-point flow towards a stretching vertical sheet, Meccanica 41 (2006) 509–518.

[29] T.R. Mahapatra, A.S. Gupta, Heat transfer in stagnation-point towards a stretching sheet, Heat Mass Transfer 38 (2002) 517–521.

[30] R. Nazar, N. Amin, D. Filip, I. Pop, Unsteady boundary layer flow in the region of the stagnation point on a stretching sheet, Int. J. Eng. Sci. 42 (2004) 1241–1253.

[31] S.R. Pop, T. Grosan, I. Pop, Radiation effects on the flow near the stagnation point of a stretching sheet, Tech. Mech. 25 (2004) 100–106.